Assessment of post-fire vegetation state dynamics in Ivan-Arakhley natural Park (Zabaikalsky Krai) using radar Sentinel 1 and optical Sentinel 2 data

Natalia Rodionova
Kotel'nikov FIRE RAS
Fryazino, Russia
rnv@sunclass.ire.rssi.ru

Irina Vakhnina
lInstitute of Natural Resouces, Ecology and Cryology SB RAS
Chita, Russia
vahnina_il@mail.ru

Tatiana Zhelibo
lInstitute of Natural Resouces, Ecology and Cryology SB RAS
Chita, Russia
Zhelibo@mail.ru

***Abstract*—The results of the analysis of multi - temporal satellite monitoring of the post-fire vegetation state dynamics in the territory of Ivan - Arakhley natural Park (Zabaikalsky Krai) after the fire in 2015 is presented using Sentinel 1 (S1) radar data and Sentinel 2 (S2) optical data. To assess the dynamics of revegetation affected by natural fire, spectral vegetation indices (VI) NDVI, ARVI, NBR, NDMI and radar vegetation index RVI are used. A positive trend has been revealed in the restoration of vegetation in the test areas of the natural Park by both optical and radar indices.**

***Keywords*—C-band radar data, multispectral optical data, vegetation cover, wildfires, vegetation indices**

I. Introduction

In Siberia, one of the highest levels of wildfire activity is observed in Zabaikalsky Krai. Vegetation renewal in this area is significantly difficult due to the arid climate. There is little precipitation, 90% of it (within 300 mm) fall during the warm period, mainly in July and August. Winters are snowless, and the soil is not moistened by snow. This leads to the fact that the region is very hot in the spring. Experts [1] found that the successful renewal of the forest is hindered by a number of reasons: 1) the high temperature of the soil on the burning, leading to the death of undergrowth, 2) lack of moisture and nutrients, leading to severe competition between plants and the grass grow, 3) repeated fires.

Remote sensing data and ground data are used to monitor forest development after a fire.

The paper [2] describes the ground - based studies of vegetation conditions on the territory of Ivan-Arakhley nature Park conducted in 2013-2014 after the grass-roots fires of 2000, 2001, 2003 and 2010. The test sites laid on the South-Eastern slopes of the Aspen ridge have characteristic forest types: rhododendron, cranberry and yernikovye leaf forests. These stands were affected by grass-roots fires of varying intensity. As a result of the study, it is shown that the natural renewal of wood species is characterized as unsatisfactory.

In mid-April 2015, severe forest fires were observed in the TRANS-Baikal region near the Beklemishev lake system. Fig. 1 (a) shows a map of fires on the territory of Osinovka for April 14, 2015 according to the ScanEx operational monitoring system, the service "Kosmosnimki - Fires" [3]. In [4], the radar images of the Sentinel 1 satellite were used to determine the ashes in this area based on the use of amplitude and texture information.

After 2015, the territories of the Ivan-Arakhley Park were not exposed to fire for four years.

This paper traces the dynamics of vegetation restoration in the 4 years since the fire in 2015 on the territory of the Ivan-Arakhley nature Park using radar and optical data Sentinel 1/2 satellites. The task is to find out whether the vegetation is being restored and how this process changes over the years.

II. Study Area

In the mountain-taiga larch landscapes of the Kondinsky district, test areas are selected for studying the dynamics of changes in plant communities (Fig. 1 (b)). The area on the Aspen ridge located in the basin of the river Osinovka, conventionally called Osinovka, the area on the Yablonovy ridge, in the basin of the river Rasmalai called "Rasmalai". Detailed descriptions of 12 test sites in Osinovka with a photo of general view of the sample areas where employees of the Institute of Natural Resources, Ecology and Cryology SB RAS worked in 2018 are given in the table.

The climate in the study area is sharply continental, a characteristic phenomenon should be noted the presence of permafrost. The ground freezes deep in winter at 1-1.5 meters and thaws slowly.

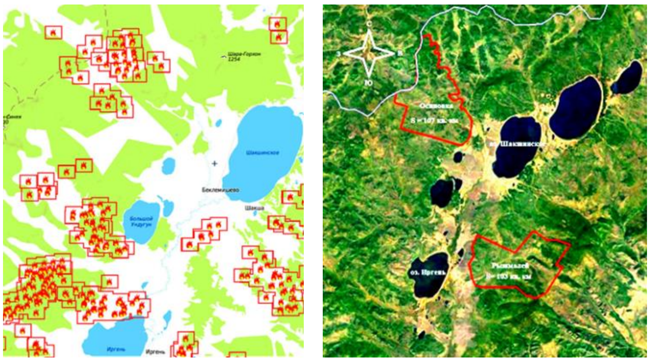

(a) (b)

Fig. 1. Fire map for 14.04.2015 according to ScanEx operational monitoring system [3] (a), the location of test areas for study the dynamics of changes in plant communities (b).

III. Input Data and Research Methods

A. Sentinel 1 radar data. Radar vegetation index

The work uses open-access Sentinel 1 radar data, IW (interferometric wide swath) mode, VV and VH polarizations, spatial resolution 10 m. All the images were pre-processed by the Sentinel-1 Toolbox and later SNAP [5]. Pre-processing included the selection of a fragment with the study area and radiometric calibration.

TABLE I. DESCRIPTION OF OSINOVKA TEST SITES

№	Coordinates	Height, m	Type of community	Violation of the territory	Photo
1	52.20855° N, 112.56738°E	1070		burn on cutting down	
2	52.20631°, 112.56490°	1029	the ernika cereal	ashes	
3	52.19739°, 112.57023°	996	the listvyaga forb	gorelnik, windfall	
4	52°12´24.9´´, 112°32´40.3´´	1053	the listvyaga Brusnichnoye	ashes, windfall	
5	52°12´42.0´´, 112°32´02.5´´	1099	the listvyaga Brusnichnoye	ashes, windfall	
6	52.18975°, 112.54653°	1051	the listvyaga forb	ashes, windfall	
7	52.19275°, 112.54384°	1021	the listvyaga forb	ashes	
8	52.19133°, 112.54929°	1026	the listvyaga omnicopy	ashes, windfall	
9	52.21100°, 112.53900°	1068	the listvyaga rhododendron	ashes, windfall	
10	52.21421°, 112.53182°	1071	the listvyaga forb	gorelnik, windfall	
11	52.20604°, 112.55075°	1044	the listvyaga Brusnichnoye	ashes, windfall	
12	52.21030°, 112.53596°	1102	the listvyaga Brusnichnoye	ashes, windfall	

S1 sessions for 26.07.2017, 02.08.2018 and 28.07.2019 were taken to determine the average value of the backscattering coefficient (BC) for the profiles for the 12 test sites studied. For comparison with the sites with burning, a background site (№13) was selected, where there was no fire in 2015, in the Northern part of lake Shakshinsky, the profile coordinates are 52.2037° N, 112.7229° E. Fig. 2 (a) shows a graph of the BC change in dB for 12 sites plus the background for 2017-2019. The BC values increased for both polarizations over the period 2017-2019. The greatest changes in the BC were observed for VH cross-polarization. For example, for site №5, the changes are 6.6 dB over two years, i.e. a significant increase in volume scattering associated with vegetation growth, whereas for VV polarization is 1.8 dB. The smallest changes in the BC VH polarization – for site №8-are less than 2 dB, this value is even less than the changes for the background profile.

The backscattering coefficient is an absolute polarimetric parameter, whereas the radar vegetation index (RVI) [6] is a relative parameter that is not very sensitive to the view angle and natural conditions. RVI is used to monitor vegetation growth using multi-temporal radar data:

$$RVI = \frac{8\sigma_{HV}}{\sigma_{HH}+\sigma_{VV}+2\sigma_{HV}} \quad (1)$$

RVI changes from 0 (smooth bare soil) to 1 as vegetation grows and is a measure of volume scattering. Sentinel 1 IW GRD mode has two polarizations VV and VH. Then under the assumption [7],

$$\sigma_{HH} \approx \sigma_{VV} \quad (2)$$

equation (1) can be represented as:

$$RVI = \frac{4\sigma_{VH}}{\sigma_{VV} + \sigma_{VH}}$$

Assumption (2) is valid for negligible interaction between soil and vegetation [8]. RVI correlates with VWC (Volumetric Water Content), LAI (Leaf Area Index) and NDVI (Normalized Difference Vegetation Index) and is poorly sensitive to natural conditions [9]. Fig. 2 (b) shows a graph of RVI changes for the test sites under study with survey dates of 26.7.17, 2.8.18, and 28.7.19. Note the significant growth of vegetation for site №5, where the RVI changed from 0.385 in 2017 to 0.99 in 2018. For the same site, an increase in the BC of 6.6 dB for VH polarization is noted above. A slightly smaller increase in RVI is obtained from site №9 with an increase in RVI of 0.5 and from site №7 with an increase in RVI of 0.35. The decrease in RVI is noted for site №8.

Fig. 3 shows images of the study area for both polarizations in RGB encoding: red-26.07.2017, green – 02.08.2018, blue-28.07.2019. All changes took place over the past years 2017-2019 on the territory of burn after the fire in 2015. This territory is allocated in figure 3 by white line. Multi-temporal radar images revealed areas of ashes. The rest of the territory has changed slightly.

B. Sentinel 2 multispectral data. Vegetation indices

The ESA Sentinel 2A satellite was launched in June 2015, and the second Sentinel 2B in March 2017. The multispectral camera has 13 spectral bands spanning from the visible and near infrared to the short wave infrared. The spatial resolution varies from 10 m to 60 m depending on the spectral band. The temporal resolution one of S2 is 10 days, and two satellites – 5 days. Image processing was performed by SNAP.

The S2 sessions for 31.07.2016, 05.08.2017, 31.07.2018, and 26.07.2019 were taken to determine the VI by profiles for the 12 sites studied. The choice of images was determined primarily by the lack of clouds for the month of July and the proximity of the dates to the dates of the radar survey. Since the territories were covered by clouds or their shadows for a number of sites on 26.07.2019, the data for the sites №5, №6, №7, №10 and №12 were replaced with data for 06.07.2019.

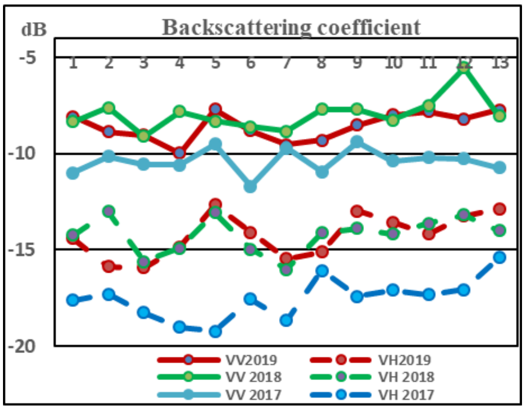

(a)

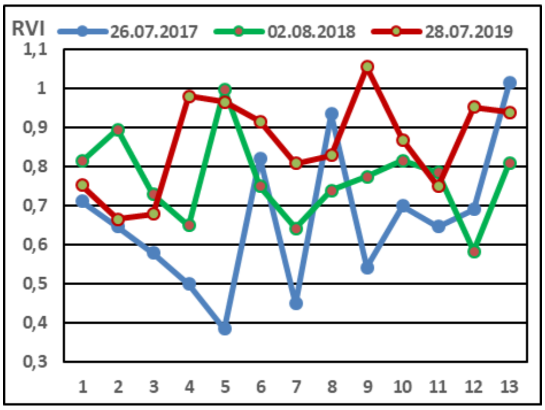

(b)

Fig. 2. Change in the backscatter coefficient (a), change in the RVI (b) for test sites over three years.

Spectral indices obtained from remote sensing optical data, such as the Normalized Difference Vegetation Index (NDVI) [10], Normalized Burn Ratio (NBR) [11] and Normalized Difference Moisture Index (NDMI) [12] and their modifications dNDVI, dNBR, dNDMI, which determine the difference of indices before and after a fire, give good results in identifying areas with damage to vegetation. Graphs based on the NBR and dNBR reflect the dynamics and nature of vegetation cover restoration in burned areas [13].

NDVI and ARVI

NDVI- VI showing the presence and state of vegetation (relative biomass):

$$NDVI = \frac{NIR - R}{NIR + R}$$

where NIR and R are the values of the reflection coefficient of the earth's surface in the NIR and Red bands. NDVI changes in the range from -1 to 1. Changes in reflectivity in the visible and NIR bands are associated with a decrease in the content of chlorophyll in the vegetative organs of shrinking trees. The absorption zone of chlorophyll in Red band of the spectrum determines the low level of vegetation reflection in the visible spectral band. Under stress, the formation of chlorophyll in plants decreases, which leads to a decrease in its absorption in the visible range and, consequently, an increase in reflectivity. In the NIR band, the reflection coefficient of green vegetation increases noticeably, reaching 45-50% [14].

Fig. 4 (a) shows graphs of NDVI changes for the test sites under study from 2016 to 2019. The NDVI values for 2019 were unexpectedly lower than for 2018 and even for 2016 for sites №5, №10, and №12. A possible reason is a number of disadvantages of the NDVI, which lead to uncertainties in its quantitative assessment. In [15], the following disadvantages were noted: non-linearity, influence of the atmosphere (water vapor and aerosols), saturation at high biomass, sensitivity to the presence of clouds, influence of soil, object geometry, influence of spectral effects (various tools). The main limitation of NDVI and similar indices is that optical sensors can only monitor a very thin layer of vegetation, and cannot provide information about woody vegetation.

One of the modifications of NDVI to account for the influence of the atmosphere is the atmospheric resistant VI ARVI (Atmospheric Resistant Vegetation Index) [16]:

$$ARVI = \frac{NIR - RB}{NIR + RB}$$

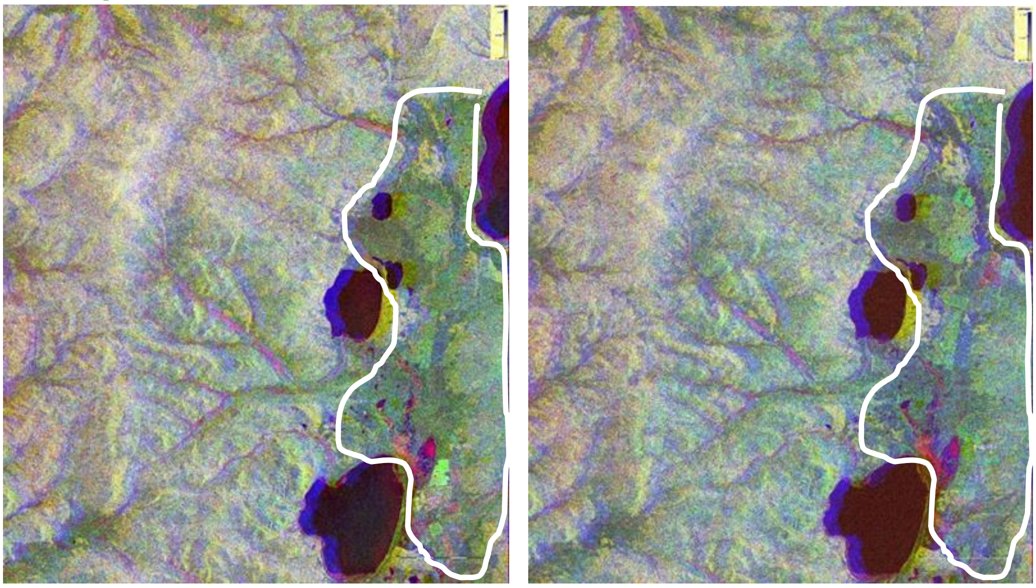

Fig. 3. Images of the study area in RGB encoding: red-26.07.17, green-2.08.18, blue-28.07.19 for VV and VH polarizations.

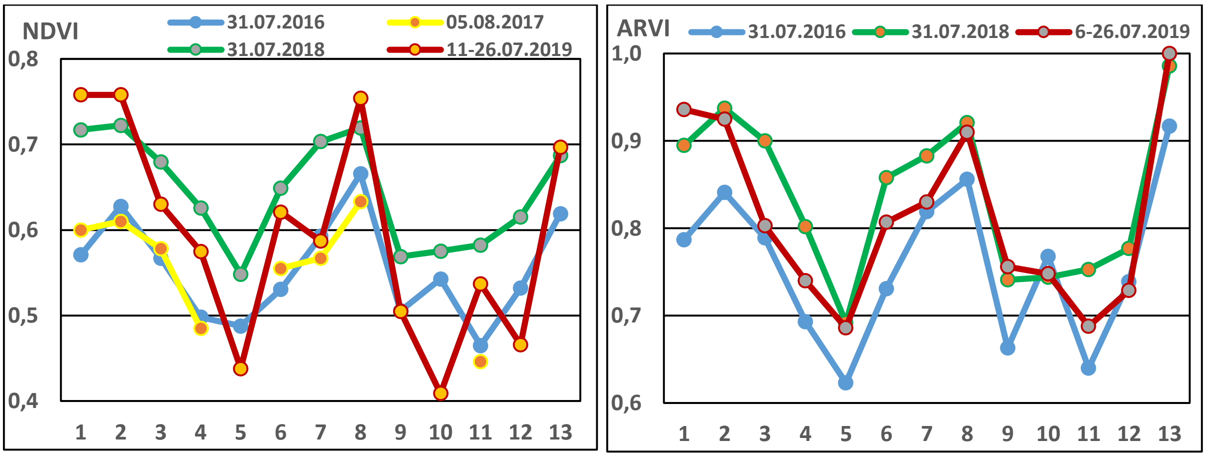

(a) (b)

Fig. 4. Changes NDVI (a) and ARVI (b) for test sites in 2016-2019.

where RB=R- γ (B-R), B is the value of the reflection coefficient in the blue range of the spectrum. This index replaces the Red band in NDVI with a combination of Red and Blue bands. This combination has self-correcting properties for atmospheric effects. ARVI variations with atmospheric opacity variations are significantly smaller than NDVI variations. The optimal value of the coefficient γ, depending on the type of aerosol, is γ =1 [16]. ARVI is 4 times less sensitive to atmospheric effects (aerosol) than NDVI [14], and its dynamic range is the same as that of NDVI. The greatest effect of using ARVI, instead of NDVI, is achieved for surfaces with vegetation rather than for soil, and for particle sizes in the atmosphere from medium to small, rather than for large particles (marine aerosols or dust). It should be noted that this index was proposed for the

MODIS sensor with bands: Blue (0.47±0.01 μm), Red (0.66±0.025 μm) and NIR (0.865±0.02 μm). Having S2 bands with wavelengths very close to the corresponding values for MODIS, namely, Blue with a central wavelength of 0.4966 μm - S2A and 0.4921 μm - S2B, Red - 0.6645 and 0.665 μm and NIR-0.835 and 0.833 μm, you can use the ARVI formula obtained for MODIS also for S2. Fig. 4 (b) shows ARVI change graphs for three dates. The use of the ARVI VI showed 1) an increase in biomass over the years since the fire for almost all test sites, 2) an increase in the saturation threshold.

NBR and NDMI

VI NBR is determined by the equation [11]:

$$NBR = \frac{\mathrm{NIR} - \mathrm{SWIR2}}{\mathrm{NIR} + \mathrm{SWIR2}}$$

where SWIR2 is the value of the reflection coefficient of the earth's surface in the Shortwave infrared spectral band. This spectral band reflects changes in the moisture content of plants, as well as changes in the structure of the canopy and the structure of leaves. The combined use of SWIR2 with NIR, which does not depend on the moisture saturation of the plant, but depends on the leaf structure, increases the accuracy of estimating the moisture content in the plant regardless of the leaf structure [17].

Fig. 5 (a) shows the NBR change graphs for the test sites for 2016-2019. Based on changes in NBR values for 2016-2019, the moisture content for all test sites, exposed to fire, increased, and remained almost the same for the background area where there was no fire.

VI NDMI is sensitive to the level of humidity in vegetation. It is used to track droughts and also indicates the level of combustible materials in fire-prone areas. VI uses the NIR and SWIR1 bands to create a coefficient designed to dim lighting and atmospheric effects:

$$NDMI = \frac{NIR - SWIR1}{NIR + SWIR1}$$

It should be noted that the author of [18] showed that a change in SWIR1 spectral band makes the largest contribution to the separation of disturbed and undisturbed forest ecosystems.

Fig. 5 (b) shows graphs of NDMI changes for the test sites in 2016-2019. The graphs in Fig. 5 (a) and (b) are very similar in the nature of changes in values. For all test sites, the vegetation humidity level increased in 2016-2019, with the least for the background site.

Based on the considered optical vegetation indices NDVI, ARVI, NBR and NDMI, we can make a general conclusion about the positive dynamics of vegetation recovery after the fire in 2015 at 12 sites under consideration in the territory of the Ivan-Arakhley nature Park. Specifically, the values of the ARVI vegetation index, which shows relative biomass, have increased for all test sites since the fire, except for site 10. The values of the NBR and NDMI indices, which reflect the presence of moisture in vegetation, increased over the post-fire years for all test sites.

IV. CONCLUSION

This paper assesses the dynamics of vegetation restoration in the territory of Ivan-Arakhley natural Park after wildfires in April 2015 using radar and optical data from Sentinel 1/2 satellites. The radar (RVI) and optical vegetation indices (NDVI, ARVI, NBR, NDMI) showed positive dynamics in the state of vegetation growth in 12 test sites in the post-fire years. Only for test site №10 the ARVI value decreased in the post-fire years.

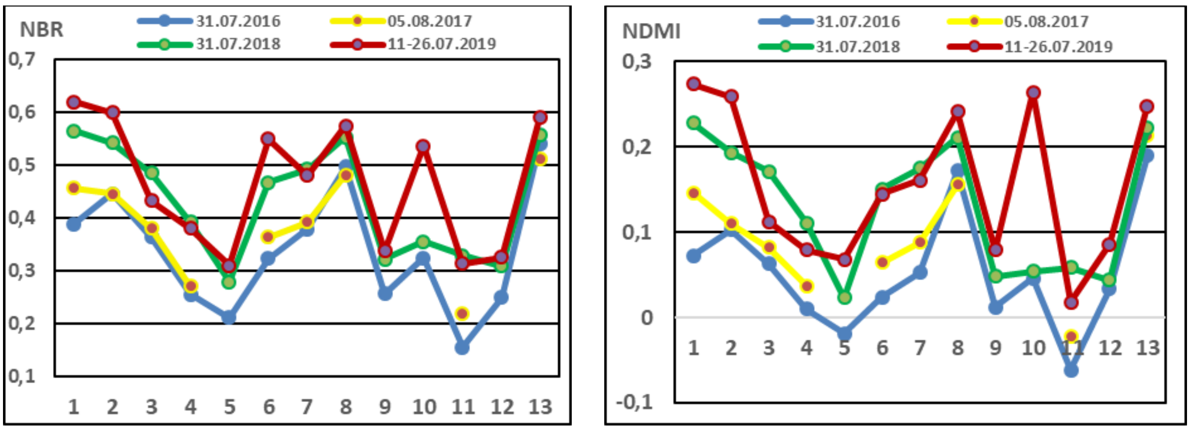

(a) (b)

Fig. 5. NBR and NDMI changes for test sites in 2016-2019.

ACKNOWLEDGMENT

The authors thank Vladimir Petrovich Makarov, Ph. D., Institute of Natural Resources, Ecology and Cryology SB RAS, for the organization of field work in the area of the Beklemishevskaya depression.

REFERENCES

[1] E.G. Shvetsov, E.A. Kukavskaya, L.V. Buryak and K. Barrett, “Assessment of post-fire vegetation recovery in Southern Siberia using remote sensing observations,” Environ. Res. Let., vol. 14, pp. 1-10, 2019. DOI: 10.1088/1748-9326/ab083d.
[2] I.V. Gorbunov, V.P. Makarov and O.F. Malyh, “Postfire vegetation state in territory Ivan-Arakhley natural park (Zabaikalsky krai),” Uspekhi sovremennogo estestvoznaniya, vol. 7, pp. 54-59, 2015.
[3] URL: http://fires.kosmosnimki.ru/.
[4] N.V. Rodionova, “Evaluation of SENTINEL 1 imagery for burned area detection in southern Siberia in spring and summer 2015,” Sovremennye problemy distancionnogo zondirovaniya Zemli iz kosmosa, vol. 13, no. 2, pp. 164-175, 2016.
[5] URL: https://sentinel.esa.int/web/sentinel/toolboxes/sentinel-1.

[6] Y. Kim and J. van Zyl, "Vegetation effects on soil moisture estimation," Proc. IGARSS, vol. 2, pp. 800-802, 2004.

[7] F. Charbonneau, M. Trudel and R. Fernandes, "Use of dual polarization and multi-incidence SAR for soil permeability mapping," Advanced Synthetic Aperture Radar (ASAR), St-Hubert Canada, 2005.

[8] M. Trudel, F. Charbonneau and R. Leconte, "Using RADARSAT-2 polarimetric and ENVISAT-ASAR dual-polarization data for estimating soil moisture over agricultural fields," Can. J. Remote Sensing**,** vol. 38, no. 4, pp. 514-527, 2012.

[9] Y. Kim and J. van Zyl, "A time-series approach to estimate soil moisture using polarimetric radar data," IEEE Trans. GRS, vol. 47, no. 8, pp. 2519-2527, 2009.

[10] J.W. Rouse, R.H. Haas, J.A. Schell and D.W. Deering, "Monitoring vegetation systems in the Great Plains with ERTS," Third ERTS Symposium NASA SP-351 I , pp. 309-317, 1973.

[11] C.H. Key and N.C. Benson, "Landscape assessment: ground measure of severity, the Composite Burn Index; and remote sensing of severity, the Normalized Burn Ratio," FIREMON: Fire Effects Monitoring and Inventory System, USDA Forest Service, Rocky Mountain Research Station, General Technical Report RMRS-GTR-164-CD: LA, pp. 1-15, 2005.

[12] E.H. Wilson and S.A. Sader, "Detection of forest harvest type using multiple dates of Landsat TM imagery," Remote Sensing of Environment, vol. 80, pp. 385-396, 2002.

[13] V.G. Bondur, M.N. Cidilina and E.V. Cherepanova, "Satellite monitoring of wildfire impacts on the conditions of various types of vegetation cover in the federal districts of the Russian Federation," Issledovanie Zemli iz kosmosa, vol. 3, pp. 13-32, 2019.

[14] S.A. Bartalev, V.A. Egorov, A.M. Krylov, F.V. Stycenko and T.S. Hovratovich, "The evaluation of possibilities to assess forest burnt severity using multi-spectral satellite data," Sovrem. problemy DZZ iz kosmosa, vol. 7, pp. 215-225, 2010.

[15] A. Huete, K. Didan and T. Miura, "Overview of the radiometric and biophysical performance of the modis vegetation indices," Remote Sens. Environ., vol. 83, no. 195, pp. 213-221, 2002.

[16] Y.J. Kaufman and D. Tanré, "Atmospherically Resistant Vegetation Index (ARVI) for EOS-MODIS," IEEE Trans. GRS, vol. 30, no. 2, pp. 261-270, 1992. DOI: 10.1109/36.134076.

[17] P. Ceccato, S. Flasse, S. Tarantola, S. Jacquemond and J. Gregoire, "Detecting vegetation water content using reflectance in the optical domain," Remote Sensing of Environment, vol. 77, pp. 22-33, 2001.

[18] E.A. Terekhin, "Detection of disturbed forest ecosystems in the forest-steppe zone using reflectance values," Computer Optics, vol. 43, no. 3, pp. 412-418, 2019. DOI: 10.18287/0134-2452-2019-43-3-412-418.